Organic LETTERS

Letter

pubs.acs.org/OrgLett

Aminorifamycins and Sporalactams Produced in Culture by a Micromonospora sp. Isolated from a Northeastern-Pacific Marine Sediment Are Potent Antibiotics

David E. Williams,[†] Doralyn S. Dalisay,[†,⊥] Jessie Chen,[‡] Elena A. Polishchuck,[‡] Brian O. Patrick,[‡] Gagandeep Narula,[§] Mary Ko,[§] Yossef Av-Gay,[§] Haoxin Li,[∥] Nathan Magarvey,[∥] and Raymond J. Andersen*[,†]

[†]Departments of Chemistry and Earth, Ocean and Atmospheric Sciences, University of British Columbia, 2036 Main Mall, Vancouver, B.C., Canada V6T 1Z1

[‡]Department of Chemistry, University of British Columbia, 2036 Main Mall, Vancouver, B.C., Canada V6T 1Z1

[§]Infection and Immunity Research Centre, University of British Columbia, 350-2660 Oak Street, Vancouver, B.C., Canada V6H 3Z6

[∥]Departments of Biochemistry and Biomedical Sciences, McMaster University, Hamilton, Ontario, Canada

[⊥]Department of Pharmacy and Gregor Mendel Research Laboratories, University of San Agustin, Iloilo City, Philippines

Supporting Information

ABSTRACT: The new ansa macrolide antibiotics **1** to **4** have been isolated from cultures of a *Micromonospora* sp. obtained from a marine sediment. Rifamycins **1** and **2** are the first natural ansa macrolides to have a 3-amino substituent. Sporalactams A (**3**) and B (**4**) are comprised of a heterocylic core **5** and a 14-membered ansa bridge that are both unprecedented. Sporalactam B (**4**) shows selective and potent inhibition of *Mycobacterium tuberculosis*.

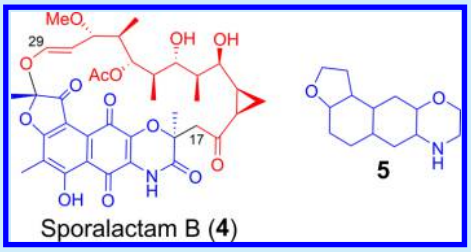

One of the major challenges facing medicine is the widespread rise in antibiotic resistance found in human microbial pathogens that cause infections in hospital and community patient populations.[1−3] The Infectious Diseases Society of America has highlighted the particularly serious resistance problem in "ESKAPE" pathogens (*Enterococcus faecium*, *Staphylococcus aureus*, *Klebsiella pneumoniae*, *Acinetobacter baumannii*, *Pseudomonas aeruginosa*, and *Enterobacter* species), calling on the research community to engage in a vigorous "10 by 20" research effort[3] that would lead to the development of 10 new clinically useful antibiotics to combat these and other pathogens by 2020. In addition to the ESKAPE pathogens, antibiotic resistance with worrying clinical implications has also been observed in *Mycobacterium tuberculosis* (*Mtb*),[4] *M. abscessus*,[5] *Escherichia coli*,[6] *Neisseria gonorrhoeae*,[7] and *Helicobacter pylori*.[8] Many of the antibiotics in clinical use are secondary metabolites (natural products) produced in culture by microorganisms, and there continues to be strong interest in exploring marine and terrestrial microbial secondary metabolism as a resource for the discovery and development of new antibacterial scaffolds.[9]

As part of an ongoing program designed to discover new antibiotics,[10−12] the EtOAc extracts of solid agar cultures of a *Micromonospora* sp. RJA4480 isolated from a marine sediment obtained at −85m in Barkley Sound, British Columbia were found to exhibit potent in vitro inhibition of MRSA and *E. coli*. Assay-guided fractionation of the extracts identified 3-amino-27-demethoxy-27-hydroxyrifamycin S (**1**), 3-amino-rifamycin S (**2**), sporalactam A (**3**), and sporalactam B (**4**) as the antibacterial components. 3-Amino-rifamycin S (**2**) has been produced by semisynthesis,[13] but no 3-amino ansa macrolide has been reported as a natural product. The 3-amino substituent in **1** and **2** significantly enhances the in vitro antibacterial potency of the rifamycin scaffold.[14] Sporalactams A (**3**) and B (**4**) contain a 1,2,6a,7,8,9,10a,11-octahydro-6*H*-furo[2′,3′:7,8]naphtho[2,3-*b*][1,4]oxazine heterocyclic core **5**, which is unprecedented in natural products or from synthesis at any oxidation state, and their 14-membered polyketide bridge has not been found before in ansa macrolides. Sporalactam B (**4**) shows potent in vitro antibacterial activity against *M. tuberculosis* in broth and is active in macrophages. Details of the isolation, structure elucidation, and biological activities of compounds **1**−**4** are presented below.

Cultures of the *Micromonospora* sp. RJA4480 (16S rRNA gene sequence GenBank accession number KY129664) were grown as lawns on solid agar containing marine medium, and the solid agar media with attached cells from mature cultures were extracted with EtOAc (Supporting Information (SI)). The combined EtOAc extracts were fractionated using sequential application of Sephadex LH20 chromatography, step-gradient Si Gel flash chromatography, and reversed-phase HPLC to give pure samples of 3-amino-27-demethoxy-27-hydroxyrifamycin S (**1**: 3.6 mg), 3-

Received: December 5, 2016
Published: February 6, 2017

DOI: 10.1021/acs.orglett.6b03619
Org. Lett. 2017, 19, 766−769

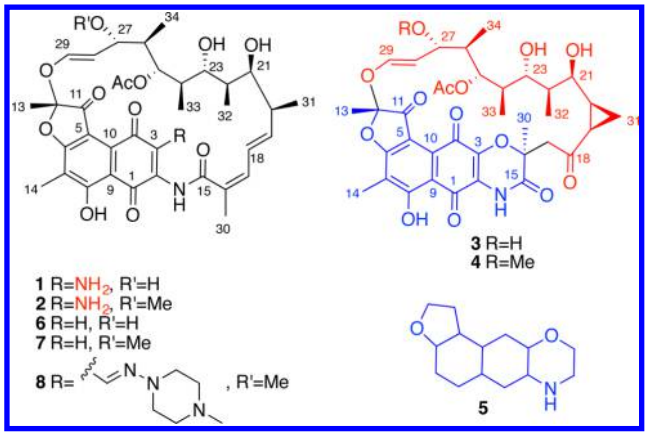

amino-rifamycin S (**2**: 0.6 mg), sporalactam A (**3**: 0.6 mg), and sporalactam B (**4**: 0.7 mg).

3-Amino-27-demethoxy-27-hydroxyrifamycin S (**1**) was obtained as optically active dark red crystals that gave a $[M + Na]^+$ ion in the HRTOFESIMS at m/z 719.2798 appropriate for a molecular formula of $C_{36}H_{44}N_2O_{12}$ (calcd for $C_{36}H_{44}N_2O_{12}Na$ 719.2792) requiring 16 sites of unsaturation. The isolated sample of **1** gave a sharp well-resolved peak when analyzed by reversed-phase HPLC using a variety of solvent systems and gave a single clean molecular ion in the HRTOFESIMS, but all of the resonances in the 1D ^1H and ^{13}C NMR spectra of **1** recorded in DMSO-d_6 were doubled (Tables 1 and 2, SI). Detailed analysis of the 1D and 2D NMR data for each of the two independent sets of peaks in the NMR spectra of **1** identified the same polyketide fragment that differed from the C-15 to C-29 fragment in rifamycin S (**7**) simply by the replacement of the C-27 OMe substituent in **7** by a C-27 OH substituent in **1** (Figure 2).[4] The remaining resonances in the ^1H and ^{13}C NMR spectra of **1** could be assigned to a fragment that was closely related to the tricyclic C-1 to C-14 fragment found in **7**. An aromatic singlet at ~δ 7.2 assigned to H-3 in rifamycin S (**7**) was missing in the ^1H NMR spectrum of **1**, and there was a new two proton singlet resonance at δ 7.56 that correlated to a nitrogen at δ −290.2 in the ^{15}NHSQC spectrum and to aromatic resonances at δ 110.2 and 178.7 in the HMBC spectrum, suggesting that **1** had an amino substituent at C-3.

The structure of **1** proposed from analysis of its NMR data was confirmed by single-crystal X-ray diffraction analysis. Interestingly, **1** crystallizes with four molecules in the asymmetric unit representing two different macrolide conformations about the O-12/C-29 and C-28/C-27 bonds. The ORTEP diagrams in Figure 1A and 1B show two of the molecules of **1** in the asymmetric unit that have the same absolute configuration but differ in the

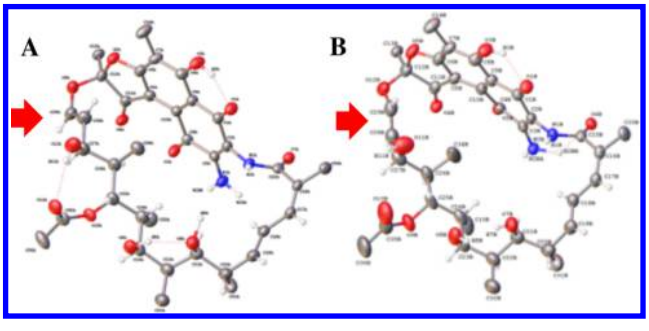

Figure 1. ORTEP diagrams of 3-amino-27-demethoxy-27-hydroxyrifamycin S (**1**). Red arrows show different conformations about the O-12/C-29 and C-28/C-27 bonds.

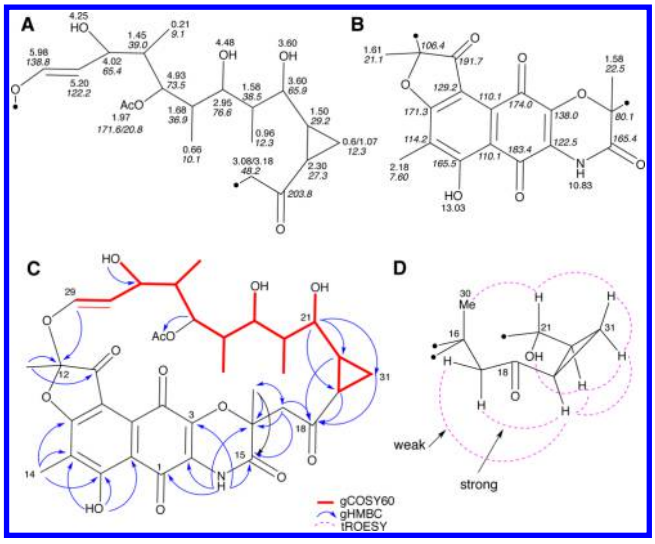

Figure 2. Summary of NMR assignments and selected COSY60, HMBC, and tROESY correlations observed for sporalactam A (**3**).

macrolide conformation. ORTEP diagrams of all four of the forms in the asymmetric unit along with overlays are shown in the SI. The existence of two macrolide conformations in the crystals of 3-amino-27-demethoxy-27-hydroxyrifamycin S (**1**) is consistent with the doubling of resonances observed in the 1D NMR spectra of **1**. The absolute configurations of the chiral centers (12*S*,20*S*,21*S*,22*R*,23*R*,24*R*,25*S*,26*S*,27*S*) were determined on the basis of the refined Flack X-parameter, [0.07(6)] (SI).

3-Amino-rifamycin S (**2**)[13,14] was identified by detailed analysis of its HRTOFESIMS and 1D and 2D NMR data (SI) that showed it differed from **1** simply by the replacement of the OH substituent at C-27 in **1** with a C-27 OMe substituent in **2**.

Sporalactam A (**3**) was isolated as a dark red glass that gave a $[M + Na]^+$ ion in the HRESIMS at m/z 734.2414 consistent with a molecular formula of $C_{36}H_{41}NO_{14}$ (calcd for $C_{36}H_{41}NO_{14}Na$, 734.2425) requiring 17 sites of unsaturation. The molecular formula of **3** differs from the molecular formula of **1** by the addition of O_2 and the loss of NH_3. Preliminary comparison of the NMR spectra recorded for **3** with those obtained for **1** and **2** suggested that the three compounds were structurally related ansa macrocycles. The resonances in the ^1H and ^{13}C NMR spectra (Table 3, SI) recorded for **3** in DMSO-d_6 were not doubled as was observed for **1** and **2**, which simplified the structure elucidation of **3**.

Analysis of the 1D $^1H/^{13}C$ and 2D HSQC, COSY, and HMBC NMR spectra revealed as shown in Figure 2 that a portion of the *ansa* chain from C-21 to C-29 and the naphthalenic nucleus from C-1 to C-14 in **3** are identical to the corresponding fragments in **1**, and that these fragments in **3** are also connected via an ether linkage between C-12 and C-29. A resonance at δ 10.83 (2-NH) in the ^1H NMR spectrum of **3** showed a correlation to a nitrogen resonance at δ −261.8 (2-N) in the ^{15}NHSQC spectrum and to carbon resonances at δ 183.4 (C-1), 122.5 (C-2), 138.0 (C-3), and 165.4 (C-15) in the HMBC spectrum, which demonstrated that the lone nitrogen atom in **3** was present as an acylamino substituent at C-2, typical of ansamycins. The C-21 to C-29 polyketide fragment, the C-1 to C-14 naphthalenic fragment, the C-2 aminoacyl substituent, and an additional ketone identified by a ^{13}C NMR resonance at δ 203.8 (C-18) accounted for 14 of the required 17 sites of unsaturation in **3**. A lack of NMR evidence for further

DOI: 10.1021/acs.orglett.6b03619
Org. Lett. 2017, 19, 766−769

unsaturated functional groups in **3** indicated there had to be three additional rings.

Further analysis of the 2D NMR data (Figure 2 and SI) established the complete constitution of sporalactam A (**3**). The H-21 resonance at δ 3.60 showed HMBC correlations to carbon resonances at δ 29.2 (CH: C-20), 27.3 (CH: C-19), and 12.3 (CH_2: C-31) and a COSY60 correlation to a proton multiplet at δ 1.50 (H-20) that was correlated to the carbon resonance at δ 29.2 (C-20) in the HSQC spectrum. Additional COSY60 correlations were observed between H-20 (δ 1.50) and resonances at δ 2.30 (H-19) and δ 0.60/1.07 (H-31/31′) that were correlated to the carbon resonances at δ 27.3 and 12.3, respectively, in the HSQC spectrum. This set of 2D correlations and the upfield chemical shifts of H-31/31′/C-31 identified a disubstituted cyclopropyl ring connected to C-21 through a C-20/C-21 bond. A methyl singlet at δ 1.58 (Me-30) showed HMBC correlations to the C-15 amide carbonyl resonance at δ 165.4, to an oxygenated tertiary carbon resonance at δ 80.1 (C-16), and to a methylene resonance at δ 48.2 (C-17) that showed HSQC correlations to the isolated two proton AB spin system at δ 3.08 and 3.18 (H-17/17′). This sequence of correlations demonstrated that the C-15 amide carbonyl was attached to the oxygenated tertiary carbon C-16, which was in turn attached to Me-30 and C-17. The H-17/H-17′ methylene protons (δ 3.08/3.18) along with the H-19, H-20, H-31′ (δ 2.30, 1.50, and 0.6, respectively) cyclopropyl protons all showed HMBC correlations to the ketone carbonyl resonance at δ 203.8 (C-18), which established that C-17 and C-19 were linked via the C-18 ketone to close the macrocyclic ring. One additional ring needed to be incorporated into the structure of **3** in order to satisfy its molecular formula. The ^{1}H NMR spectrum of **3** was missing an aromatic singlet resonance that could be assigned to H-3. Therefore, connecting the C-16 oxygenated tertiary carbon (δ 80.1) and C-3 via an ether linkage provided the final ring and completed the constitution of sporalactam A (**3**) (Figure 2).

Sporalactam B (**4**) was isolated as a dark red glass that gave a $[M + Na]^+$ ion at m/z 748.2556 in the HRTOFESIMS appropriate for a molecular formula of $C_{37}H_{43}NO_{14}$ (calcd for $C_{37}H_{43}NO_{14}Na$, 748.2581) that differed from the molecular formula of **3** simply by the addition of CH_2. The NMR spectra obtained for sporalactam B (**4**) (SI) only differed from the NMR spectra obtained for sporalactam A (**3**) by the replacement of a resonance at δ 4.25 assigned to the exchangeable 27-OH in **3** with a methyl singlet at δ 2.94 that correlated in the HMBC spectrum to a carbon resonance at δ 76.8, assigned to C-27 in the spectra of **4**. Therefore, sporalactam B (**4**) was the 27-methoxy analogue of **3**, the same relationship observed between compounds **1** and **2**.

Sporalactams A (**3**) and B (**4**) are biogenetically related to the cyclopropyl-containing antibiotic tolypomycin Y (**8**).[15] The absolute configuration of tolypomycinone (**9**),[16] a degradation product of tolypomycin Y, has been determined by single-crystal X-ray diffraction analysis.[16] We have assigned the absolute configurations at C-12 and in the C-21 to C-29 ansa bridge fragments of sporalactams A (**3**) and B (**4**) to be the same as those

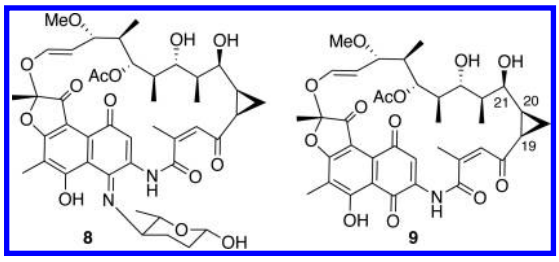

determined by single crystal X-ray diffraction analysis for the co-occurring 3-amino-27-demethoxy-27-hydroxyrifamycin S (**1**) (Figure 1) and tolypomycinone (**9**)[16] on the basis of a presumed common biogenesis for **1**, **3**, **4**, and **9**. With the C-21 configurations in **3** and **4** assigned as *S* by biogenetic arguments, the ROESY data obtained for **3** and **4** (Figure 2) confirmed that the absolute configurations at C-19 and C-20 were the same 19*R*,20*S* configurations reported for tolypomycinone (**9**).[16] The Me-30 resonances in both **3** and **4** (δ 1.58 and 1.56, respectively) showed strong ROESY correlation to the respective H-21 resonances (δ 3.60 and 3.45) (Figure 2). MM2 calculations of the lowest energy conformations of the sporalactam B (**4**) C-16 epimers (SI Figures SI2A and SI2B) clearly showed that the observed Me-30 to H-21 ROESY correlations in **3** and **4** are only possible if the C-16 absolute configuration is *S*. Therefore, the complete absolute configurations of **3** and **4** have been assigned as 12*S*,16*S*,19*R*,-20*S*,21*S*,22*R*,23*R*,24*R*,25*S*,26*S*,27*S*.

Macrolides **1**−**4** and the two reference compounds 27-demethoxy-27-hydroxyrifamycin S (**6**) and rifamycin S (**7**) were evaluated for in vitro broth culture antimicrobial activity against a panel of human pathogens and for their ability to inhibit *M. tuberculosis* growing intracellularly in macrophage cells[17] (Tables 1 and SI4). Comparison of the MIC_{90}'s for **1** and **2** with the reference rifamycins **6** and **7** lacking only the 3-amino substituent (Tables 1 and SI1) shows that the 3-amino substituent significantly enhances the potency of these antibiotics against MRSA, *E. coli*, and *M. tuberculosis*. Sporalactams A (**3**) and B (**4**) are much less active against MRSA and *E. coli* than are **6** and **7**, but sporalactam B (**4**) has activity comparable to **6** against *M. tuberculosis*, both in broth and in macrophages.

Rifampin (**10**), rifamixin, and other rifamycin analogs are clinically important antibiotics that are widely used as treatments for tuberculosis (TB) and traveler's diarrhea (caused by *E. coli*).[4] As part of the development of the rifamycins into clinically useful drugs, there have been many investigations of the SAR for this antibacterial pharmacophore coupled with NMR and X-ray analysis of the conformations required for effective inhibition of bacterial RNA polymerase, the molecular target.

The conformational studies of rifamycin S (**7**) show that the molecule behaves much like a basket, represented by the naphthalenic core, with a handle (Latin handle = ansa), represented by the polyketide fragment attached at C-2 and C-12.[4] Flexibility is only observed at the C-2 amide attachment point and around the C-28/C-27 and O-12/C-29 bonds (Figure 1). A conformation in which one plane containing the naphthalenic core and the oxygen atoms at C-1 and C-8 and a second plane containing the C-21 and C-23 carbon atoms and OHs are parallel to each other and all four oxygen atoms are pointing in the same direction (Figure 1) is optimal for binding to their target RNA polymerase. Synthetic analogues of rifamycin S (**7**) with a simple primary amine (e.g., **2**) or other nitrogen substituent at C-3 (e.g., **10**), which can make a hydrogen bond with the C-15 amide carbonyl oxygen atom or sterically lock the amide conformation at C-2 into the optimal macrolide shape for binding to RNA polymerase, show significantly enhanced antibacterial potency.[14] Discovery of the natural 3-amino rifamycins **1** and **2** in RJA4480 cultures reveals that nature has also taken advantage of this SAR improvement in rifamycin antimicrobial activity.

The heterocyclic core and 14-membered bridge in the sporalactams are unprecedented in ansa macrolides, although the ansa fragments of **3** and **4** contain the C-18 to C-29 bridge segment found in tolypomycin Y (**8**) and tolypomycinone (**9**). Tolypomycinone (**9**) has been reported to have only weak

DOI: 10.1021/acs.orglett.6b03619
Org. Lett. 2017, 19, 766−769

Table 1. In Vitro Broth Culture and Intracellular[17] MIC_{90}'s in μM (Full Panel in SI)

	1	2	3	4	6	7
MRSA	0.0009	0.0008	7.0	1.8	0.03	0.07
E. coli	0.0003	0.0001	1.8	0.4	0.07	0.001
Mtb	0.0009	0.0008	0.8	0.06	0.04	0.006
Mtb in macrophages	0.7	0.4	9−30	3−9	3−10	0.7

antibacterial activity.[16] X-ray analysis of the conformation of **9** revealed that the plane containing the C-1 and C-8 oxygen atoms and the plane containing the C-21 and C-23 carbon atoms and OHs are not parallel, but rather sit at an angle to each other such that the C-21 and C-23 OHs point into the naphthalenic ring, and this has been proposed as a reason for its lack of potent antimicrobial activity.[16] The conformation of the sporalactams **3** and **4** has not yet been determined by X-ray diffraction analysis, but the combination of different orientations of the bridge attachment points in **3** and **4** (C-12 and C-16) compared with **7** and **9** (C-12 and C-2) and the shorter polyketide bridge (14- versus 17-membered) are expected to result in a conformation that differs from both the rifamycins and tolypomycinone. A calculated MM2 energy minimized conformation for sporalactam B (**4**) (SI Figure SI2C) shows that the plane containing the C-1 and C-8 oxygen atoms and the heterocyclic core is roughly perpendicular to a plane containing the C-21 and C-23 carbons and OH groups, in contrast to previous predictions of the requirements for potent rifamyicn inhibition of RNA polymerase activity. In keeping with the expected and calculated difference in shape between **4** and **6**/**7**, their antimicrobial activities are also different. Sporalactam B (**4**) is much less active than rifamycins **6** and **7** against MRSA and *E. coli* (≥25 fold), but is equi-potent with **6** against *M. tuberculosis* in broth and in macrophages (Table 1).

Genomic DNA of RJA4480 was sequenced, and the rifamycin analogue cluster was identified by PRISM (SI). A total of 17 homology searches using the rifamycin gene cluster from RJA4480 against the known rifamycin producer *Amycolatopsis mediterranei* S699 revealed an identical biosynthetic gene cluster split between six contigs. The pairwise alignment revealed a percent identity for nucleotides of 81%. The main differences between the two clusters were the position of the P450 gene and the lack of a rifamycin MFS transporter gene. The discovery of these rare rifamycin analogues provides evidence that even small differences in a well-studied biosynthetic cluster can lead to structural diversity and improved bioactivities.

The worldwide TB disease burden is exacerbated by the widespread occurrence of XDR-TB, *M. tuberculosis* strains that are virtually untreatable with current medicines. A pipeline of new anti-TB drugs that would shorten the duration of treatment, be effective against MDR-TB and latent TB in macrophage cells, and have lower toxicity is urgently needed.[4] Sporalactam B (**4**) has a new ansa macrolide template comprised of an unprecedented heterocylic core and ansa bridge components. It is active against Mtb in macrophage cells but is not toxic to the macrophages at the effective anti-Mtb dose. Therefore, sporalactam B (**4**) represents a promising new candidate for the anti-TB drug pipeline.

■ ASSOCIATED CONTENT

Supporting Information

The Supporting Information is available free of charge on the ACS Publications website at DOI: 10.1021/acs.orglett.6b03619.

Experimental details; NMR spectra and NMR assignments for **1**−**4**; experimental details for X-ray analysis of **1**; details of genomic analysis (PDF)

Crystallographic data (CIF)

■ AUTHOR INFORMATION

Corresponding Author

*E-mail: raymond.andersen@ubc.ca.

ORCID

Yossef Av-Gay: 0000-0002-9547-0237

Raymond J. Andersen: 0000-0002-7607-8213

Notes

The authors declare no competing financial interest.

■ ACKNOWLEDGMENTS

Financial support was provided by grants from the Natural Sciences and Engineering Research Council of Canada (R.J.A.), CIHR (N.M., R.J.A., Y.A.), and British Columbia Lung Association (Y.A.). The authors thank M. le Blanc (EOAS, UBC) for technical assistance.

■ REFERENCES

(1) Meredith, H. R.; Srimani, J. K.; Lee, A. J.; Lopatkin, A. J.; You, L. *Nat. Chem. Biol.* **2015**, *11*, 182−188.

(2) Boucher, H. W.; Talbot, G. H.; Benjamin, D. K., Jr; Bradley, J.; Guidos, R. J.; Jones, R. N.; Murray, B. E.; Bonomo, R. A.; Gilbert, D. *Clin. Infect. Dis.* **2013**, *56*, 1685.

(3) Boucher, H. W.; Talbot, G. H.; Bradley, J. S.; Gilbert, D.; Rice, L. B.; Scheld, M.; Spellberg, B.; Bartlett, J. *Clin. Infect. Dis.* **2009**, *48*, 1.

(4) Aristoff, P. A.; Garcia, G. A.; Kirchhoff, P. D.; Showalter, H. D. H. *Tuberculosis* **2010**, *90*, 94.

(5) Nessar, R.; Cambau, E.; Reyrat, J. M.; Murray, A.; Gicquel, B. *J. Antimicrob. Chemother.* **2012**, *67*, 810.

(6) Kim, J. H.; Sun, H. Y.; Kim, T. H.; Shim, S. R.; Doo, S. W.; Yang, W. J.; Lee, E. J.; Song, Y. S. *Medicine* **2016**, *95*, e4663.

(7) Hill, S. A.; Masters, T. L.; Wachter, J. *Microb. Cell* **2016**, *3*, 371.

(8) Hu, Y.; Zhang, M.; Lu, B.; Dai, J. *Helicobacter* **2016**, *21*, 349.

(9) Moloney, M. G. *Trends Pharmacol. Sci.* **2016**, *37*, 689.

(10) Ratnaweera, P. B.; Williams, D. E.; Patrick, B. O.; de Silva, E. D.; Andersen, R. J. *Org. Lett.* **2015**, *17*, 2074.

(11) Centko, R. M.; Ramon-Garcia, S.; Taylor, T.; Patrick, B. O.; Thompson, C. J.; Miao, V. P.; Andersen, R. J. *J. Nat. Prod.* **2012**, *75*, 2178.

(12) Zoraghi, R.; Worrall, L.; See, R. H.; Strangman, W.; Popplewell, W. L.; Gong, H.; Samaai, T.; Swayze, R. D.; Kaur, S.; Vuckovic, M.; Finlay, B. B.; Brunham, R. C.; McMaster, W. R.; Davies-Coleman, M. T.; Strynadka, N. C.; Andersen, R. J.; Reiner, N. E. *J. Biol. Chem.* **2011**, *286*, 44716.

(13) Dampier, M. F.; Whitlock, H. W. *J. Am. Chem. Soc.* **1975**, *97*, 6254.

(14) Marsili, L.; Pasqualucci, C. R.; Vigevani, A.; Gioia, B.; Schioppacassi, G.; Oronzo, G. *J. Antibiot.* **1981**, *34*, 1033.

(15) Kishi, T.; Harada, S.; Asai, M.; Muroi, M.; Mizuno, K. *Tetrahedron Lett.* **1969**, *10*, 97.

(16) Brufani, M.; Cellai, L.; Cerrini, S.; Fedeli, W.; Vaciago, A. *Mol. Pharmacol.* **1978**, *14*, 693.

(17) Sorrentino, F.; Gonzalez del Rio, R.; Zheng, X.; Matilla, J. P.; Torres Gomez, P.; Hoyos, M. M.; Perez Herran, M. E.; Mendoza Losana, A.; Av-Gay, Y. *Antimicrob. Agents Chemother.* **2016**, *60*, 640.

DOI: 10.1021/acs.orglett.6b03619
Org. Lett. 2017, 19, 766−769